Wollschlaeger, J.; Roettgers, R.; Petersen, W.; Wiltshire, K.H.:

**Performance of absorption coefficient measurements for the in situ determination of chlorophyll-a and total suspended matter**

In: Journal of Experimental Marine Biology and Ecology (2014) Elsevier

DOI: 10.1016/j.jembe.2014.01.011

# Performance of absorption coefficient measurements for the *in situ* determination of chlorophyll-*a* and total suspended matter

Wollschläger, Jochen[1]*; Röttgers, Rüdiger[1]; Petersen, Wilhelm[1]; Wiltshire, Karen H.[2]

[1] Helmholtz-Zentrum Geesthacht, Centre for Materials and Coastal Research, Institute of Coastal Research, Max-Planck-Str. 1, 21502 Geesthacht, Germany

[2] Alfred Wegener Institute for Polar and Marine Research, Kurpromenade, 27498 Helgoland Germany

*corresponding author: Jochen.Wollschlaeger@hzg.de

**Abstract**

The concentration of chlorophyll-*a* ([chl-*a*]) and total suspended matter ([TSM]) are important parameters in biological oceanography. [Chl-*a*] is a commonly used proxy for estimating phytoplankton biomass while [TSM] also includes detrital material and mineral particles and thus influences light attenuation and photosynthetic activity in the water column.

For characterizing the distribution (patchiness) of both parameters adequately over a longer time period, fast and effective measurement methods are required that can also be applied *in situ* or continuously. Thus, alternatively to direct determination of [chl-*a*] and [TSM], optical proxy values are often measured. The PSICAM is an integrating cavity approach for measuring absorption coefficients of water constituents with high precision which can be used also continuously (flow-through-PSICAM). In this study, the performance of these absorption measurements for [chl-*a*] and [TSM] determination was evaluated and compared with the performance of traditional approaches using chl-*a* fluorescence and turbidity measurements.

Data were collected in the German Bight (North Sea) in 2010 and 2011. For [chl-*a*], fluorescence measurements are compared with pigment absorption coefficient values at a

wavelength of 676 nm ($a_{\Phi\ 676\ nm}$), while the [TSM]-proxies were turbidity and particle absorption at 700 nm ($a_{p\ 700\ nm}$). As reference data, HPLC-determined [chl-*a*] and gravimetrically determined [TSM] were used.

Our results showed linear relationships between [chl-*a*] and fluorescence or $a_{\Phi\ 676\ nm}$, respectively. Coefficients of determination ($R^2$) were in a range of 0.71 to 0.88, with the higher values related to the absorption measurements. Furthermore, it was demonstrated that fluorescence underestimates [chl-*a*] depending on ambient photosynthetically active radiation (PAR). Linear relationships were also observed between [TSM] and its optical proxies with $R^2$ values between 0.93 and 0.98. Turbidity measurements appeared to be influenced to a certain extent by the physical properties of the suspended material, resulting in a slightly higher variability than the $a_{p\ 700\ nm}$ measurements.

Absorption measurements turned out to be promising optical proxies for determining [TSM] and [chl-*a*] due to their lower variability compared with the other proxies. This improved accuracy could be already partially achieved also for continuous measurements. Moreover, a combination of the different optical methods has the potential to provide additional information besides concentration, such as the source of TSM in the water or physiological condition of the phytoplankton.

**Keywords:** chlorophyll-*a*, total suspended matter, fluorescence, absorption, German Bight, evaluation of flow through-PSICAM

## 1. Introduction

The North Sea is, like most shelf and coastal seas, a highly productive ecosystem fostered by relatively shallow waters and a constant supply with nutrients by river discharge (Ducrotoy, et al., 2000). The impact of e.g. fishing, shipping, pollution and energy production is high today and is likely to further increase in future. By enabling the detection of long-term changes driven by this increasing utilization as well as by climate changes, time series like

the Helgoland Roads (Wiltshire, et al., 2010) or the Continuous Plankton Recorder (Reid, et al., 2003) have shown their value. Information on phytoplankton, the basis of the marine food web, is of particular importance, as changes in this part of the ecosystem also affect higher trophic levels. In this context, phytoplankton biomass is a key parameter and needed for productivity and ecosystem model calculations. A commonly used and early introduced approach for its estimation is the measurement of the concentration of the major algal pigment chlorophyll-*a* (referred to as [chl-*a*] hereafter) in the water (Harvey, 1933; Mineeva, 2011). Although the relationship between [chl-*a*] in the water and phytoplankton biomass is not constant but varies with species composition (Llewellyn and Gibb, 2000), acclimatization to light conditions (Falkowski and Owens, 1980; Llewellyn, et al., 2005), or developmental stage (Llewellyn and Gibb, 2000), it allows reasonable estimates about phytoplankton without tedious microscopic observations. In addition to [chl-*a*], total suspended matter concentration in the water (hereafter referred to as [TSM]) is another important parameter to measure, because it is governing e.g. the underwater light regime and thereby influencing phytoplankton photosynthetic activity.

Today, the most accurate method for direct [chl-*a*]-measurement is high performance liquid chromatography (HPLC), while for [TSM] it is gravimetry. Both approaches require a high degree of manual handling and are restricted to the analysis of discrete samples from fixed stations or occasional research cruises. Hence, although accurate, they often provide only insufficiently detailed information because of the lack in spatial and temporal resolution. Furthermore, the high effort in the analyses hampers the establishment and maintenance of time series covering these parameters.

Measurement of optical proxy values can be an alternative to the measurement of the parameters itself. Although less accurate than direct measurements, they offer a cost-effective, fast and convenient way to estimate a variety of parameters relevant to marine researchers, and many of the available methods can be applied on an *in situ* or continuously basis (Moore, et al., 2009). While [TSM] is traditionally determined via light scattering in the water by turbidimeters (Sternberg, et al., 1974; Vant, 1990), [chl-*a*] is commonly determined

via its fluorescence (Lorenzen, 1966; Ostrowska, et al., 2000). Because the intensity of the fluorescence signal depends amongst others on [chl-*a*], it allows estimates about the phytoplankton biomass in a given sample. Although the signal can be accurately calibrated against HPLC-determined [chl-*a*], the calibration is not stable over longer periods of time as well as in changing environmental conditions (Wiltshire, et al., 1998; Beutler, et al., 2002; Beutler, et al., 2004). The variability in the ratio between fluorescence and [chl-*a*] is caused e.g. by variations in the physiological state of the cells, in species composition, and in the variable fluorescence yield itself in dependence of the actual and short-time historic light conditions (Falkowski and Kiefer, 1985; Cunningham, 1996; Chekalyuk and Hafez, 2011). Despite this uncertainties and due to their convenience, approaches based on fluorescence were widely used for mapping of horizontal and vertical phytoplankton distributions (e.g. Uehlinger, 1985; Seppälä and Balode, 1998; Wiltshire, et al., 1998; Muylaert, et al., 2006).Due to the relative simplicity of turbidity and fluorescence measurements, the respective instruments are also predestined to be used in unattended, long term-measurement systems to further increase data resolution in time and space. For example, they are mounted on time series stations (Badewien, et al., 2009), or in FerryBoxes aboard on ships of opportunity (Fleming and Kaitala 2006; Lips, et al., 2007; Petersen, et al., 2008; Petersen, et al., 2011) to monitor TSM and phytoplankton dynamics in real-time.

Alternatively to turbidity and fluorescence, [TSM] and [chl-*a*] can be determined by measuring absorption coefficients (Yentsch and Phinney, 1989; Bricaud, et al., 1995; Wollschläger, et al., 2013). With respect to chl-*a*, the advantage is given by measuring a physical parameter of the cells instead of a more physiological value as it is the case for fluorescence, making [chl-*a*] determination potentially more accurate. This is especially important when data were obtained from unattended devices (satellites, gliders, FerryBoxes) where direct [chl-*a*] measurements for calibration are not necessarily available. However, measurement of spectral absorption coefficients in seawater is more complicated than measurement of chl-*a* fluorescence or turbidity. With the exception of some coastal areas, the content of absorbing material in seawater is relatively low and additional light loss due to

scattering on particles requires the application of empirical correction procedures. Several instruments are available for the determination of absorption coefficients (Pegau, et al., 1995; Moore, et al., 2009), and some of them address the problem of low concentration by using larger linear cuvettes or by using liquid wavelength capillary cells (Kirkpatrick, et al., 2011). Nevertheless, the bias due to scattering remains. In this context, devices based upon the use of integrating cavities (Fry, et al., 1992; Kirk, 1997; Pope, et al., 2000; Röttgers, et al., 2005) are promising, as they are independent of the need for scattering corrections, highly sensitive due to a long optical path length, and still compact in design. Recently, efforts have been made to adapt these systems also for continuous measurements and tests *in vitro* (Musser, et al., 2009) and *in situ* (Wollschläger, et al., 2013) have been performed.

In this study, we evaluated the performance of absorption coefficient measurements for the determination of [TSM] and [chl-*a*] by comparison with traditional methods like fluorescence and turbidity measurements. Because of the aforementioned advantages, the absorption coefficients were determined using an integrating cavity approach, a point source integrating cavity absorption meter (PSICAM). As mentioned, the possibility of obtaining continuous measurements is crucial; for this reason, also the performance of a flow-through-version of this device was tested (ft-PSICAM). Aim was to evaluate whether potential advantages of absorption coefficient measurements for the determination of [TSM] and [ch-*a*] could also be achieved with continuous measurements.

## 2. Materials and Methods

### 2.1 Discrete sampling and continuous measurements

Data were collected on several cruises with the R.V. ‘Heincke’ in 2010 and 2011 in the German Bight, North Sea (Fig. 1; tab. 1). At the hydrographic stations (dots in figure 1), discrete samples were taken from depths of around 4 to 5 meters using a sampling rosette (SBE 32, Sea-Bird Electronic, Inc.) equipped with seven 9-L Niskin sampling bottles (Hydrobios, Germany). The water was transferred into 10-L PE containers and processed

subsequently for measurements of salinity, temperature, chl-*a*, turbidity, TSM, and absorption of water constituents. Continuous measurements of chl-*a* fluorescence and turbidity were performed by a FerryBox system as described in Petersen et al. (2011). The water intake for the FerryBox was in the moon pool of the research vessel at ca. 4 m depth, thus widely comparable to the sampling depth for the discrete measurements. Continuous measurements of water constituent absorption were performed on the cruises in April and June 2011 using a flow-through-PSICAM (ft-PSICAM) as described in Wollschläger et al. (2013). The water for these measurements was provided from a bypass of the FerryBox water supply. This ensured that both devices got the same water samples and the results were comparable. From the continuous datasets, values for the cruise stations were extracted according to the corresponding time stamps.

### 2.2 Determination of chlorophyll-*a* by HPLC

Concentration of chl-*a* was measured by high performance liquid chromatography (HPLC). Water samples (1-5 L) were filtered through pre-combusted GF/F filters (Whatman, USA, Ø 47 mm), subsequently, the filters were shock-frozen in liquid nitrogen and stored at -80 °C. Later in the laboratory, the pigments were extracted from the filters with 100 % acetone for 24 h at -30 °C (Wright, et al., 1991; modified). The extracts were transferred into 2 ml glass vials and simultaneously cleaned from particles by passing them through 0.2 µm syringe filters (regenerated cellulose, Spartan, A13). The separation and analysis of the pigments was carried out by a HPLC system from JASCO (Japan) using the method described in Zapata et al. (2000).

### 2.3 Determination of total suspended matter by gravimetry

Concentration of total suspended matter was determined by filtration of 1-8 L of the water sample through pre-combusted, pre-washed and pre-weighted GF/F filters (Whatman, USA, Ø 47 mm). Previously to usage, the filters were wet with purified water to avoid saturation of the rim with sea water during filtration. This was done in order to reduce the amount of salt

that cannot be washed out of the filter afterwards (Stavn, et al., 2009). Additionally at each cruise, already filtered and therefore particle-free seawater was applied on empty filters like real samples, and the average mass increase due to the remaining salt was determined. It was subtracted from the mass values of all samples of the particular cruise before calculating total suspended matter concentration gravimetrically (in mg/L; see Stavn et al. 2009 for details).

### 2.4 Measurement of optical proxy-values

#### 2.4.1 Chlorophyll-*a* fluorescence and turbidity

Chl-*a* fluorescence was continuously measured with SCUFA-II-sensors (Turner Design, USA) mounted in the FerryBox system. Calibration of the sensor was performed by the manufacturer. Sensitivity was checked previously to the cruise by using a solid standard provided by the manufacturer. The same sensor was also used for continuous turbidity determination using a nephelometric method measuring light scattering at an angle of 90°. For turbidity, the sensor was calibrated before the cruises in the laboratory using different suspensions of formazine in a range of 0.5 to 35 formazine nephelometric units (FNU). The turbidity of these suspensions were determined with a calibrated Hach 2100N IS turbidimeter (Hach, USA). The linear relationship between the SCUFA-II and the laboratory instrument was strong in all cases with $R^2 > 0.99$. For comparison with data from discrete samples, corresponding fluorescence and turbidity values were extracted from the continuous data set based on time of the sampling. In addition, manual turbidity measurements of samples have been done onboard using a Hach 2100P ISO turbidimeter (Hach, USA).

In preliminary analysis, an offset was visible –despite calibration– for both the turbidity and the fluorescence data measured with the SCUFA-II. After the cruises, for correction of these offsets, purified water was measured to obtain zero-values for both parameters. These values were then subtracted from the corresponding data. Since the fluorescence measurements are temperature depended, the purified water was maintained at 5 and 15 °C, because these temperatures were representative for the water measured in spring and

summer/autumn, respectively. For turbidity, a mean value of 0.2 nephelometric turbidity units (NTU) was measured, for fluorescence a mean value of 0.55 and 0.54 arbitrary units (AU) for 5 °C and 15 °C, respectively. However, it should be noted that this correction was not sufficient for a complete elimination of the offsets.

### 2.4.2 Spectral absorption coefficient determination

Discrete absorption measurements were made using a PSICAM as described in Röttgers et al. (2005) and Röttgers & Doerffer (2007). It is referred to as 'conventional PSICAM' in the following. The only change in the described setup was the use of a Hamamatsu C10083CA mini-spectrometer (Hamamatsu, Japan) during the cruises in April and June 2011. The theoretical background as well as the equations for the calculation of spectral absorption coefficients or cavity wall reflectivity is given elsewhere (Kirk, 1997; Leathers, et al., 2000). Measurements of the cavity wall reflectivity for calibration of the PSICAM were performed daily in triplicates according to Röttgers et al. (2005) using an always freshly prepared solution of the dye nigrosine, purified water (>18.2 MOhm) as reference and 0.1 % NaOCl solution (Riedel de Haën, Germany) for cleaning. Spectral absorption coefficients of the nigrosine solution were determined in advance using liquid waveguide capillary cells (path lengths: 0.5 and 2 m; WPI, USA), again with purified water as reference. Prior to their use, both solutions were adapted to the same temperature in a water bath. Sample measurements with the conventional PSICAM were also performed in triplicate, with a reference measurement previous to each sample. Subsequent to the sample measurement, the cavity was rinsed with purified water for cleaning and then the reference was measured again. Temperature for both was recorded and used together with the determined salinity (measured with a WTW 330i portable conductivity sensor; WTW, Germany) for correction of variations in pure water absorption due to temperature and salinity differences between sample and reference (Röttgers and Doerffer, 2007).

Continuous measurements of spectral absorption coefficients were performed taking advantage of a custom-made ft-PSICAM. Its setup as well as the measurement, the cleaning

and the calibration procedure is described in Wollschläger, et al., 2013. Calibration was performed daily; sample water was measured every 5 seconds and averaged over one minute. Since reference measurements were only performed at stations (in intervals of one to eight hours), spectral absorption coefficients on a transect line were calculated using linearly interpolated reference values based on the data measured on the stations at the beginning and the end of the transect. Correction of the coefficients for the influence of salt and temperature were done using temperature and salinity data obtained from the FerryBox. To maintain the performance of the system, the ft-PSICAM was cleaned in the same way as during calibration at every station. Nevertheless, the continuously obtained absorption coefficients were distorted by small contaminations and changes in the reference signal and were therefore corrected using discrete data of the conventional PSICAM (see also Wollschläger, et al., 2013). The particulate absorption coefficient at 700 nm ($a_{\mathrm{p\ 700\ nm}}$) served as a proxy value for [TSM], while for [chl-*a*] the estimated absorption coefficient of phytoplankton pigments at 676 nm ($a_{\Phi\ 676\ \mathrm{nm}}$) was used. $a_{\mathrm{p700\ nm}}$ is identical with total absorption of water constituents at this wavelength, assuming the contribution of both CDOM and pigments is negligible in this region. $a_{\Phi\ 676\ \mathrm{nm}}$ was estimated by subtracting $a_{\mathrm{p700\ nm}}$ from total absorption of water constituents at 676 nm. For details, see Wollschläger, et al., 2013.

**2.5. Additional data sets**

In the evaluation of chl-*a* determination by fluorescence and absorption, additional datasets were used. The concentration of CDOM was qualitatively estimated by fluorescence using a Cyclops-7 sensor (WETLabs, USA) mounted in the FerryBox. Furthermore, for the cruises in April and June 2011, data about photosynthetic active radiation (PAR) were obtained from the hydrographic time series station ‘Wattenmeer’ (Badewien, et al., 2009; Reuter, et al., 2009).

253

254 **3. Results & Discussion**

255 **3.1 Station measurements**

256 The first step in the evaluation of the different optical proxies for [TSM] and [chl-*a*]
257 determination was the comparison of the respective data obtained at the cruise stations with
258 the corresponding reference data ([TSM] determined gravimetrically and [chl-a] measured by
259 HPLC). Figures 2 and 4 as well as table 2 show the respective correlations. The observed
260 values of [TSM] and [chl-*a*] span roughly two orders of magnitude, with the lower values
261 sampled in the more offshore regions and the higher values near the coast. For [TSM], most
262 of the data (77 %) were below 5 g/m$^3$, while for [chl-*a*], 87 % were below a concentration of 5
263 µg/L. Turbidity was determined manually using the Hach turbidimeter and continuously by
264 the SCUFA-II. The latter was also used for chl-*a* fluorescence measurements. Particle
265 absorption coefficients at 700 nm ($a_{p\ 700\ nm}$) and pigment absorption coefficients at 676 nm ($a_{\Phi}$
266 $_{676\ nm}$) were measured manually with the conventional PSICAM and continuously with the ft-
267 PSICAM.

268

269 **3.1.1 Total suspended matter determined at cruise stations**

270 In all cases, statistically significant linear relationships between the respective optical proxy
271 value and [TSM] were observed, but the variability in the data was different for the four
272 methods: The strongest correlation was obtained for the PSICAM measurements of $a_{p\ 700\ nm}$
273 ($R^2$= 0.98; Fig. 2 E), followed by the Hach turbidity measurements ($R^2$= 0.95 Fig. 2 A) and the
274 continuously obtained optical proxy values ($R^2$= 0.94 for the ft-PSICAM measurements and
275 $R^2$= 0.93 for the SCUFA-II; Fig. 2 C, G). Thus, the manually measured optical proxies
276 allowed a slightly more stable determination of [TSM] than the continuously obtained data,
277 what is also supported by the standard error of the slope of the respective fits given in table
278 2. This was expected, since the continuous measurements were performed under less
279 controlled conditions compared to the manual ones.

Although the higher coefficient of determination and the lower error of the slope indicate a better performance of the absorption-based approach for the manual measurements, the same was not achieved for the continuous measurements. While the $R^2$-values were nearly identical, the error of the slope was higher for the ft-PSICAM measurements than for those performed with the SCUFA-II. Partly, this higher variability could be a statistical effect caused by the considerably lower sample size and range in the data of the continuous absorption measurements. But logarithmic transformation of the data (Fig. 2 B, D, F, and H) revealed increased scattering around the applied linear fits below [TSM] < 3 g/m³. Although observable for all instruments, it was especially high for the ft-PSICAM and probably the reason for the higher error of the slope. Thus, by now, the measurements of the ft-PSICAM should be treated with caution at such low [TSM].

One reason for the variable performances of the methods for [TSM]-determination are the different measurement errors of the instruments used. The relative error of the various methods in dependence of the measured [TSM] up to 10 g/m$^3$ is shown in figure 3. For both manual and continuous turbidity measurements, the averaged error of the slope obtained from the sensor calibrations was considered as measurement error of the instruments, including errors due to manual handling (Hach turbidimeter: 0.249; SCUFA-II: 0.368). The error associated with $a_{p\ 700\ nm}$ varied with the value of the respective measurement, since it was a combination of the error in wall reflectivity determination and precision of the instrument (~2 % and 0.001 m$^{-1}$ for the conventional PSICAM; Röttgers and Doerffer, 2007, for the ft-PSICAM ~5 % and 0.007 m$^{-1}$; unpublished data). Uncertainties in the gravimetrically determination of [TSM] itself were composed from errors in determination of the mass retained on the filter (average 0.003 mg), in the salt-offset (average 0.3 mg) as well as from errors in the determination of the filtered volume (average 0.4 %). The latter depended on the amount of TSM in the water, thus the related error was quite variable for the different samples. However, the contribution of the gravimetrically [TSM] determination to variations in the linear relationships can be considered as minor. Generally, instrumental errors increased

307 at [TSM] < 3 g/m³ (Fig. 3), indicating that they were primarily responsible for the observed
308 variations in the relationships between [TSM] and optical proxies at low values.
309 In cases where instrumental errors are small, observed variability in the relationship between
310 the respective optical proxy and [TSM] can also be caused by a different susceptibility to
311 natural variability in the optical properties of the investigated particles. Turbidity and particle
312 absorption are not only functions of [TSM], but also of particle size-distribution and origin
313 (e.g. organic or inorganic; Babin, et al., 2003; Babin and Stramski, 2004; Astoreca, et al.,
314 2012). A possible manifestation of this effect can be seen in the data displayed in figure 2 A.
315 Based on the calibration of the instrument, the slope of the correlation between [TSM] and
316 turbidity was expected to be close to 1. This was not the case, apparently caused by some
317 onshore stations of the September cruise in 2010, which showed relatively low turbidity
318 values although there were high [TSM] present (empty circles marked with arrows). Since the
319 relative measurement errors were generally low at high values (compare figure 3), these data
320 points might be 'outliers' because of differing scattering properties of the TSM present at
321 these stations. Possibly, the storm event occurring during this time caused re-suspension of
322 larger particles than usually present, which are less efficient light scattering per mass than
323 smaller particles (Stramski, et al., 2007; Wozniak, et al., 2010). In contrast, $a_{p\ 700\ nm}$ seemed
324 to be much less influenced by the properties of TSM, because in figure 2 E, the respective
325 stations of September 2010 appeared not as outliers. But also in the continuously measured
326 turbidity data, they were not as clearly distinguishable from the other stations as in the
327 manual measurements. It can be speculated that the large particles were only aggregates of
328 smaller ones, which were disrupted by the impeller pump of the FerryBox. This would have
329 made the particles measured more uniform and thus masking existing anomalies in particle
330 size distribution.
331
332 **3.1.2 Chlorophyll-*a* determined at cruise stations**
333 The correlation of [chl-*a*] with the measurements of the optical proxy values resulted in
334 statistically significant linear relationships (Fig. 4, tab. 2). Despite the correction applied on

the fluorescence measurements (see 2.4.1), still an offset in the data remained (0.547 +/- 0.092 AU). Possibly, an insufficient temperature correction of the sensor was the reason, or an incorrect separation of the excitation light from the emission light by the filter of the instrument, which created a signal even if no chlorophyll was present in the sample. However, linear correlations with [chl-*a*] were in general stronger for the absorption than for the fluorescence measurements, and as for TSM-determination, the manual measurements (Fig. 4 E) performed better than the continuous measurements (Fig. 4 G). The slightly higher error in the slope for ft-PSICAM measurements compared to those of the SCUFA-II can be related to the smaller number of measurements performed. Differences in the offset between the fits for the manual and the continuous obtained $a_{\Phi\ 676\ nm}$ data were only of low statistical significance (p= 0.08 derived from a t-test). Probably, the higher value for the continuous measurements was caused by the lack in high [chl-*a*] measured by the ft-PSICAM, what distorted the regression line. However, considering the offsets as negligible small, the fits were forced through zero in the following. This assumption is realistic, because chlorophyll-related absorption should be zero in the absence of chlorophyll, and led to identical slopes for both PSICAMs (0.0182 +/-0.0004 for manual $a_{\Phi\ 676\ nm,}$ and 0.0179 +/- 0.0008 for continuous $a_{\Phi\ 676\ nm}$, p= 0.7 according to a t-test). The relative error of the slope changed to 2.2 % and 4.5 %, respectively. In order to emphasize the smaller values of which the dataset consists to a majority, also the logarithm of the data was taken and fitted in a linear way. In this case, the coefficient of determination for the $a_{\Phi\ 676\ nm}$ measurements increased (Fig. 4 F, H), while it decreased for the fluorescence measurements (Fig. 4 B) because of high scattering in the data at smaller values. In summary, the stronger linearity in the relationship obtained for both the normal and the log-data, especially at lower [chl-*a*], indicated that in general $a_{\Phi\ 676\ nm}$ is a more accurate proxy for [chl-*a*] than *in situ* chl-*a* fluorescence.

The weaker performance of the fluorescence measurements might be caused on the one hand by an influence of water turbidity on the fluorescence signal (TurnerDesigns, 2004), but on the other hand also by its strong link to phytoplankton physiology (Falkowski and Kiefer, 1985). Therefore, it is influenced by a variety of parameters, e.g. the absorption properties of

363 photosystem II, which are determined by the pigment composition of the cells (Hoepffner and
364 Sathyendranath, 1991). Although principally species specific, this composition can also vary
365 due to long term adaptation of the cells to certain light conditions (Yentsch and Yentsch,
366 1979; Soohoo, et al., 1986; Lutz, et al., 2001). Additionally, self-shading of the chloroplasts,
367 the so-called 'pigment-packaging' (Duysens, 1956; Morel and Bricaud, 1981; Kirk, 1994), has
368 an impact on light absorption and therefore the amount of energy which is supplied to the
369 photosystem. Furthermore, the fluorescence yield itself, which reflects the proportion of
370 absorbed light energy that the cell uses for photochemistry, is also variable. It is discussed to
371 be influenced by the nutrient status of the cells (Kiefer, 1973b; Parkhill, et al., 2001), as it can
372 have an impact on the general condition of the photosynthetic apparatus and its enzymes.
373 Other factors are non-photochemical quenching mechanisms which allow a short-term
374 acclimatization to ambient light conditions. They can be triggered by ambient light (Szabo, et
375 al., 2005) or a diel rhythm (Prézelin and Ley, 1980). Influence of light acclimatization on the
376 fluorescence signals is also indicated for the data obtained in this study: When considering
377 only the fluorescence values measured during the night, when the cells were some kind of
378 'dark-adapted' (Fig. 4 C, D), the variability in the data was much lower compared to that
379 observable in figure 4 A and B (the value shown in brackets was considered as an outlier
380 and omitted from the calculation).
381 The –compared to the fluorescence signal– smaller variability of the $a_{\Phi\ 676\ nm}$ measurements
382 can be explained by the fact that they are only influenced by variations in the chl-*a* specific
383 absorption properties, which take place on comparably long timescales. They emerge from
384 the pigment packaging effect and the variable pigment composition of phytoplankton which
385 also affect fluorescence (see above). However, pigment composition changes are only of
386 importance if absorption measurements were conducted in the blue region of the light
387 spectrum, where also other pigments absorb in addition to chl-*a*. For measurements in the
388 red absorption maximum of chl-*a*, as were done for this study, they can be widely neglected,
389 because only chl-*a* and –to a lesser extent– chlorophyll-*b* and phycobilines absorb there.
390 According to HPLC measurements, chlorophyll-*b* concentration was mostly below 20 %

(mean value: 6 %) of that of chl-*a* in this study, and no blooms of cryptophytes or cyanobacteria containing phycobilines were observed. Thus, in most cases, the whole absorption at 676 nm can be considered due to chl-*a*, attributing nearly all natural variability observed in the relation between [chl-*a*] and $a_{\Phi\ 676\ nm}$ to the pigment packaging effect. For this reason, the accuracy of [chl-*a*] determination using the absorption-based approach is –with exception of instrumental errors– in the first line limited by natural variability which is inherent in the phytoplankton due to the packaging effect. Absorption is influenced by fewer factors than fluorescence, what explains the better performance of the PSICAM-based measurements.

### 3.2. Continuous measurements

In order to evaluate the continuous measurement systems not only by means of the station data, also the transect measurements were compared. Only transects of the cruises in April and June 2011 were used, since for the other no ft-PSICAM data were available. The optical proxy data were converted to [TSM] and [chl-*a*] using the appropriate linear equations for the respective instrument shown in table 2 (based on the non-logarithmized data). As the offset was negligible for the absorption coefficient- based relationships and it is more realistic to assume zero absorption at the absence of TSM or chl-*a*, the fits were forced through zero previously to the calculation (resulting in no alteration in the slope for TSM and a minimal change in the slope to 0.018 for chl-*a*).

#### 3.2.1 Total suspended matter determined on transects

The resulting time series for calculated [TSM] of different origin are shown in figure 5. Although the occasionally occurring negative [TSM] do not comply with reality but were a result from turbidity values below the offset, they were nevertheless included in the graph to show the relative progression of the data. In general, this progression was quite similar for the values calculated from both optical proxies, but there were also noticeable differences (e.g. 10th April, 12th April or large parts of the June cruise). Although most of the differences

were visible at low [TSM] where the variation of the instruments was relatively high (compare 3.1.1), they appeared not be caused by simple scattering, but more likely due to systematic errors. One potential error could be related to the calculation procedure of the absorption coefficients during the transect measurements: In contrast to the stations, where reference values were measured, they were interpolated in a linear way during the transect measurements between two stations (compare 2.4.2). The assumption of a linear development of the reference values was necessary for calculation of absorption coefficients from the continuous measurements. In reality, however, it is likely that short-time fluctuations in reference light intensity occurred due to instabilities in the light source or contaminations of the cavity. Although the influence of these fluctuations is difficult to quantify, it could be an explanation for the peak-like deviations of the continuous absorption-based [TSM] (Fig. 5 A, 10th-12th April). To avoid this in the future, reference measurements have to be performed more frequently.

In part, this might be also an explanation for some of the deviations visible in figure 5 B (June cruise). But here, some differences often regarded only the absolute values while the general progression of the data was similar between both [TSM] determination approaches. They were caused by the fact that a relationship obtained over several cruises instead of a cruise-specific one was used for calculating [TSM]. Comparing figure 2 C, it can be estimated that a fit applied only to the values of this cruise (black squares) would have a smaller slope compared to that calculated in the figure. The manually taken turbidity data from this cruise did not differ in a similar way from those of the other cruises (Fig. 2 A). Therefore, the systematically underestimation of turbidity by the SCUFA-II during this cruise indicated a problem with its calibration, or the sensor has been contaminated during the cruise.

Another possibility is of course that the deviations in the calculated [TSM] resulted not necessarily from problems with the sensors, but could be at least in part due to the aforementioned different optical properties of the suspended material. But at such low [TSM], where most of the deviations where observed, it is likely that potential natural variation was masked by variation due to the instrumental errors. Thus, for further comparison of the

turbidity- and absorption-based approach, additional data from areas with high [TSM] (estuaries, tidelands) would be useful. When such data were available, such measurements of $a_{p\ 700nm}$ and turbidity in parallel would be interesting to evaluate if variations in the ratio of both proxies can be attributed to differences in the nature of the suspended material.

### 3.2.2 Chlorophyll-*a* determined on transects

The [chl-*a*] time series resulting from the conversion of the optical proxy data for the two cruises investigated are shown in figure 6 A. As for TSM, negative values for the fluorescence derived [chl-a] result from fluorescence values smaller than the offset and were retained to document the relative progression of the data.

The progressions of both [chl-*a*] datasets were generally in good agreement, but frequently the absolute values were considerably different. This can be explained due to the higher variability of fluorescence compared to chl-*a* absorption. To a certain extent, light acclimatization (probably by non-photochemical quenching) of the phytoplankton played a role and resulted in a reduction of the fluorescence signal at high light intensities (Abbott, et al., 1982). This led to an underestimation of the fluorescence-based [chl-*a*] compared to the absorption-based [chl-*a*]. These light-induced differences can be seen in figure 6 B, where the relation of [chl-*a*] derived from both optical proxies is shown together with the photosynthetically active radiation (PAR) measured outside the water for the respective period. During night, the relation was close to 1 for most of the time, indicating a comparable performance of both methods in determining [chl-*a*]. But when PAR increased during the day, the relation increased to values above 8, caused by a drop in the fluorescence signal. This observed fluorescence quenching at the sea surface around noon is a typical feature that alters the fluorescence / [chl-*a*] ratio (Kiefer, 1973a; Loftus and Seliger, 1975; Babin, et al., 1996).

When light availability is reduced as in the presence of high turbidity or high CDOM values (Fig. 6 C) the relationship did not or only weakly increase, although PAR is high. Thus, it can be concluded that the observed peaks were indeed light induced and not because of an

inherent diel rhythm of the cells. This demonstrates that even if chl-*a* fluorescence is a more variable proxy than $a_{\Phi 676\ nm}$ with respect to [chl-*a*] determination, the simultaneous measurement of both parameters can be used to obtain additional information about the status of the phytoplankton.

## 4. Summary and conclusion

It was shown that [TSM] and [chl-*a*], two important parameters in biological oceanography, can be reasonably well measured using optical proxy values (turbidity, fluorescence and absorption coefficients). However, especially for spatially and temporally large heterogeneities (as we have in the German Bight when conducting long-term measurements), the absorption-based approach was indicated as being more reliable. For both [TSM] and [chl-*a*] the relationship to the corresponding absorption coefficient ($a_{p700\ nm}$ and $a_{\Phi 676\ nm}$) was more stable over the different seasons than it was to the respective traditional optical proxy, with the difference being more pronounced for chl-*a*. This was also the case for coefficients obtained continuously with the ft-PSICAM, although the variability was higher compared to the data obtained manually with the conventional PSICAM. The weaker performance of the turbidity and fluorescence-based approach was attributed to a higher susceptibility to variations in the investigated material. An influence of ambient PAR on [chl-*a*] determined via fluorescence was demonstrated.

Although allowing a more robust determination of [TSM] and [chl-*a*], continuous absorption measurements based on the PSICAM principle are by now less convenient than *in situ* chl-*a* fluorescence or turbidity measurements. Thus, for some scientific questions which do not need the higher accuracy, this approach might be too sophisticated. For other questions, e.g. the validation of remote sensing data or productivity calculations, it might be desirable and worth the effort. Furthermore, the ft-PSICAM has, since it is only a first attempt to use the PSICAM principle for continuous measurements, potential for further improvement in the future, namely achieving accuracy comparable to the high precision of conventional PSICAM measurements and a more convenient use by automation.

Moreover, devices like the PSICAM and the ft-PSICAM measure not only the absorption coefficients important for [chl-*a*] and [TSM] determination, but those of the whole visible spectrum. Such data could be used for the discrimination and identification of phytoplankton groups, what would be an additional set of valuable information for a variety of ecological questions. Therefore, it is important to put further effort in the improvement and development of such systems for reliable, high frequency measurement of water constituent absorption coefficients in the whole visible light spectrum.

**Acknowledgements**

This work was performed in the course of the EU-PROTOOL-project (ENV.2008.3.1.6.1 Development of automated sensing technologies for estuaries, coastal areas and seas). We would like to thank Kerstin Heymann at the Helmholtz-Zentrum Geesthacht for the HPLC-analysis of the water samples and the gravimetric measurements of TSM. We also thank Thomas H. Badewien and Lars Holinde from the ICBM (Institute for Chemistry and Biology of the Marine Environment) of the University of Oldenburg for providing PAR-data for the time of the relevant cruises. Thank goes also to the reviewers which helped to improve the quality of the manuscript.

**Table / figure captions**

Tab. 1: Time of the different cruises and number of stations sampled.

| cruise | date | no. of stations |
|---|---|---|
| September 2010 | 14th – 20th | 19 |
| April 2011 | 5th – 12th | 33 |
| June 2011 | 16th – 22th | 38 |
| September 2011 | 15th – 20th | 24 |

Tab. 2: Equations of linear fits shown in figure 2 and 5. P>0.05 in all cases according to t-tests.

| device | equation | standard error of slope [%] | fig. | equation (log data) | standard error of slope [%] | fig. | n |
|---|---|---|---|---|---|---|---|
| Hach | y= 0.011+0.869x | 2.3 | 2A | y= -0.097+1.042x | 2.7 | 2B | 97 |
| SCUFA-II | y= 0.684+0.366x | 2.7 | 2C | y= -0.033+0.674x | 3.5 | 2D | 100 |
| PSICAM | y= 0.001+0.016x | 1.3 | 2E | y= -1.784+0.987x | 2.2 | 2F | 98 |
| ft-PSICAM | y= -0.001+0.015x | 4.2 | 2G | y= -1.832+0.893 | 9.9 | 2H | 42 |

| device | equation | standard error of slope [%] | fig. | equation (log data) | standard error of slope [%] | fig. | n |
|---|---|---|---|---|---|---|---|
| SCUFA-II | y= 0.547+0.422x | 6.2 | 5A | y= -0.023+0.566x | 7.8 | 5B | 110 |
| SCUFA-II (night) | y= 0.649+0.498x | 10.6 | 5C | y= 0.087+0.502x | 13.3 | 5D | 21 |
| PSICAM | y= 0.004+0.017x | 3.5 | 5E | y= -1.687+0.901x | 3.1 | 5F | 110 |
| ft-PSICAM | y= 0.011+0.016x | 7.1 | 5G | y= -1.634+0.844x | 5.6 | 5H | 50 |

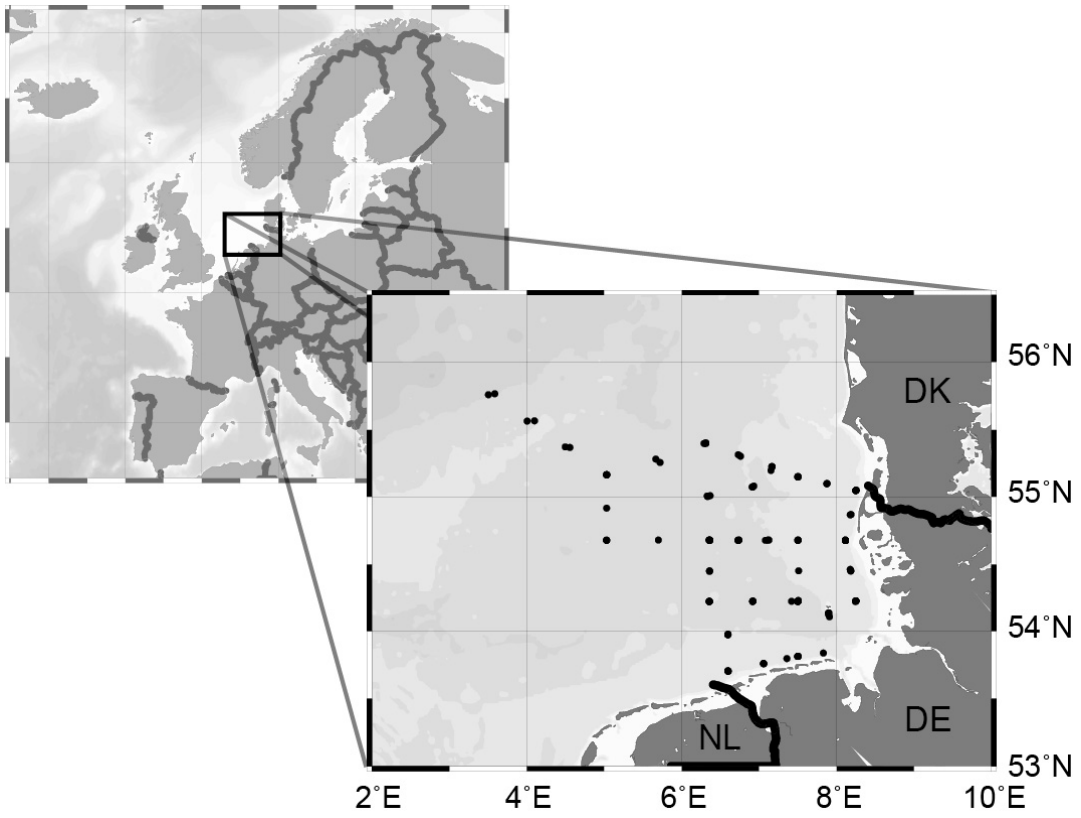


Fig. 1: Stations of the different cruises in the German Bight. Transects were carried out between the stations in different order, depending on weather conditions on the respective cruise. Different shades of grey represent the depth profile of the area (light areas = shallow, dark areas = deep). DE = Germany, DK = Denmark, NL = Netherlands. The map is based on Ocean Data View Software (Schlitzer 2012).

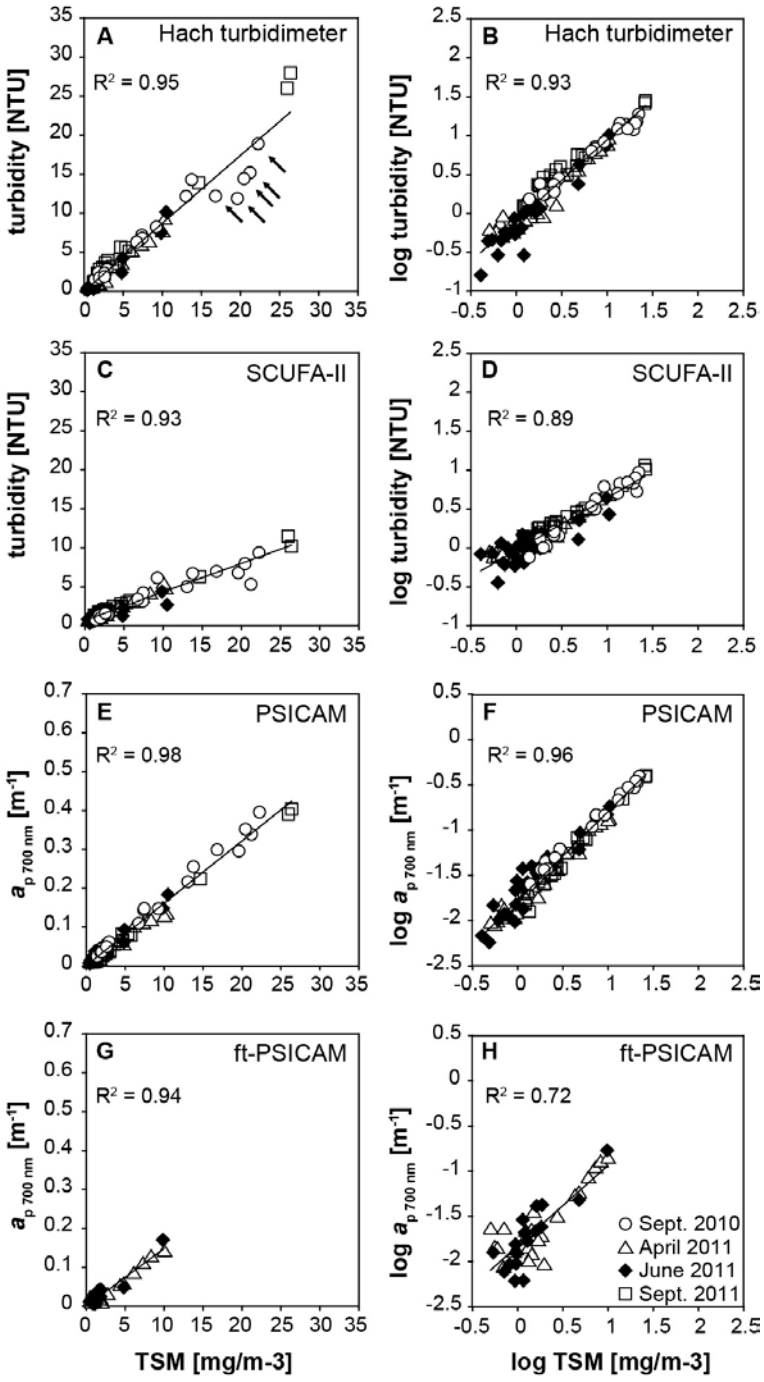


541

542 Fig. 2: Correlations between gravimetrical determined [TSM] and optical proxy values. (A, B)
543 Turbidity measured with the Hach turbidimeter, (C, D) turbidity measured with the SCUFA-II
544 (E, F) $a_{p\ 700\ nm}$ obtained by the conventional PSICAM, (G, H) $a_{p\ 700\ nm}$ obtained by the ft-
545 PSICAM. Note that the panels on the right side display the data as logarithmic values.
546 Arrows in (A) mark stations with low turbidity in relation to the measured [TSM].

547

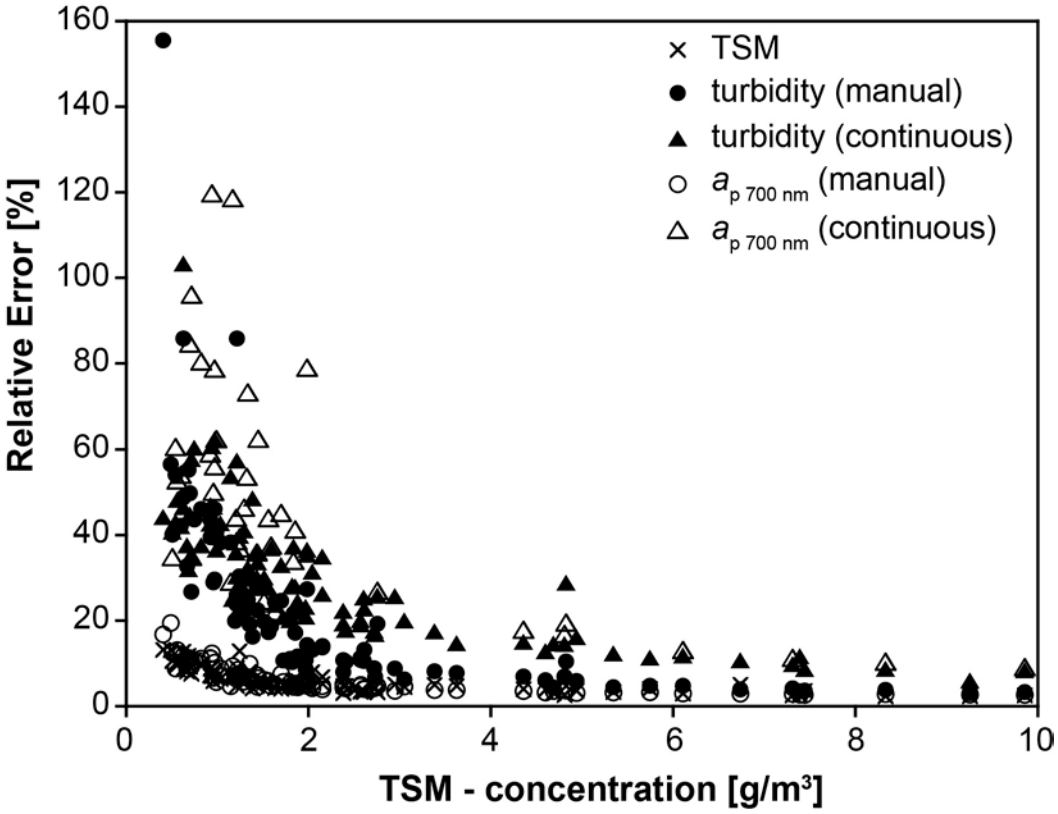


548

549 Fig. 3: Relative error of the different methods for [TSM] determination (gravimetry, turbidity

550 measurements and absorption measurements) as a function of [TSM].

551

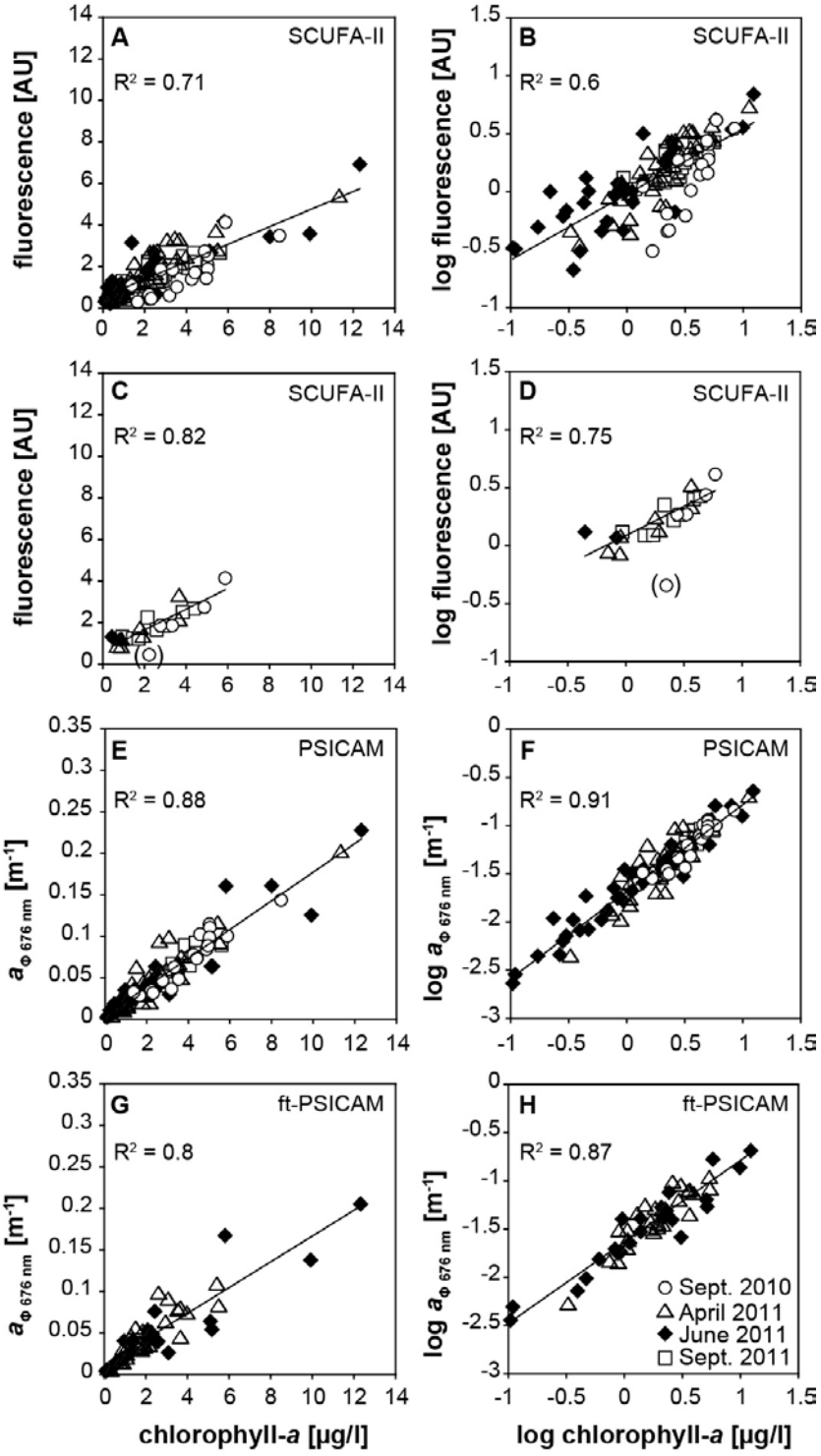


552

553 Fig. 4: Correlations between [chl-*a*] measured by HPLC and optical proxy values. (A, B)

554 Fluorescence measurements, (C, D) fluorescence measurements made after sunset, (E, F)

555 $a_{\Phi\ 676\ nm}$ obtained by the conventional PSICAM, (G, H) $a_{\Phi\ 676\ nm}$ obtained by the ft-PSICAM.

556 Note that the panels on the right side display the data as logarithmic values.

557

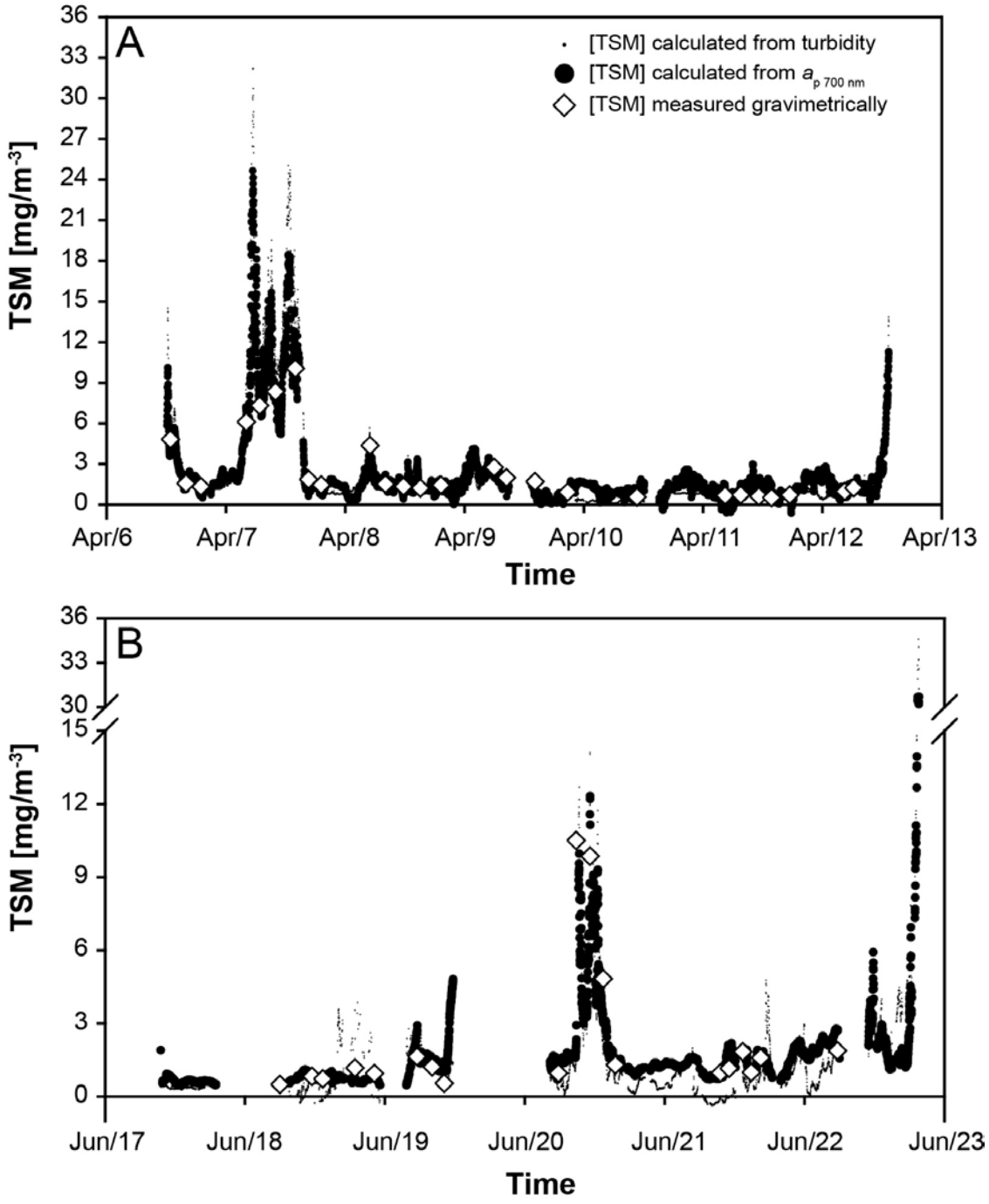


558

559 Fig. 5: Time series of [TSM] calculated from continuous turbidity and $a_{p700\ nm}$ measurements

560 taken in April 2011 (A), and June 2011 (B). Gravimetrically determined values are shown for

561 comparison.

562

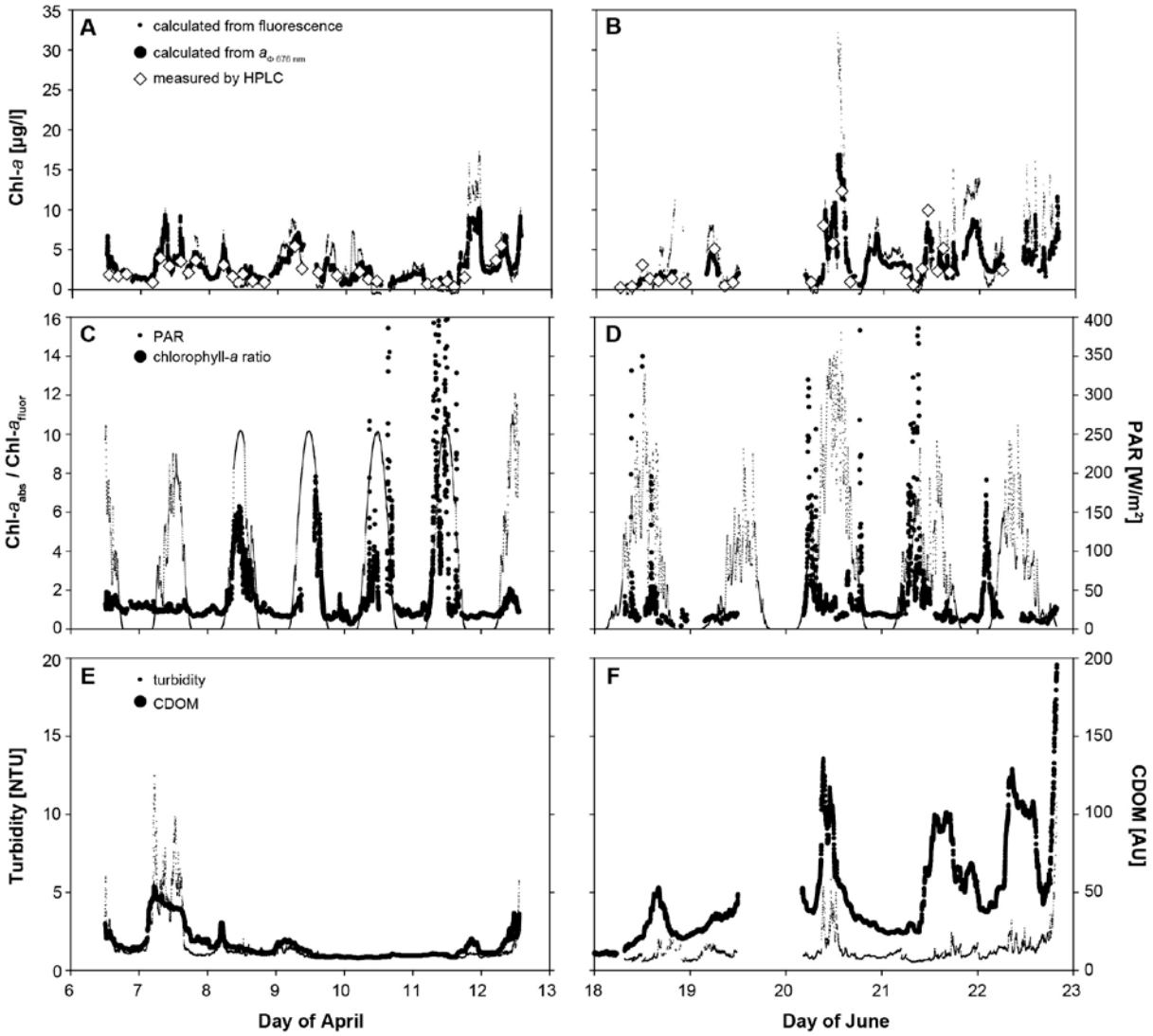


Fig. 6: Time series of the cruises in April 2011 (left) and June 2011 (right). (A, B) [chl-*a*] derived from fluorescence, $a_{\Phi\,676\,nm}$ and HPLC; (C, D) Relation of [chl-*a*] calculated from both proxies in dependence of PAR; (E, F) turbidity and CDOM for the respective time period. The legends on the left panels apply also for the respective right panels.

570

571 **References**

572 Abbott, M.R., Richerson, P.J., Powell, T.M., 1982. In situ response of phytoplankton
573 fluorescence to rapid variations in light. Limnol. Oceanogr. 27(2), 218-225.
574 Astoreca, R., Doxaran, D., Ruddick, K., Rousseau, V., Lancelot, C., 2012. Influence of
575 suspended particle concentration, composition and size on the variability of inherent
576 optical properties of the Southern North Sea. Continental Shelf Research 35, 117-
577 128.
578 Babin, M., Stramski, D., 2004. Variations in the mass-specific absorption coefficient of
579 mineral particles suspended in water. Limnol. Oceanogr. 49(3), 756-767.
580 Babin, M., Morel, A., Gentili, B., 1996. Remote sensing of sea surface Sun-induced
581 chlorophyll fluorescence: Consequences of natural variations in the optical
582 characteristics of phytoplankton and the quantum yield of chlorophyll a fluorescence.
583 Int. J. Remote Sens. 17(12), 2417-2448.
584 Babin, M., Morel, A., Fournier-Sicre, V., Fell, F., Stramski, D., 2003. Light scattering
585 properties of marine particles in coastal and open ocean waters as related to the
586 particle mass concentration. Limnol. Oceanogr. 48(2), 843-859.
587 Badewien, T.H., Zimmer, E., Bartholomä, A., Reuter, R., 2009. Towards continuous long-
588 term measurements of suspended particulate matter (SPM) in turbid coastal waters.
589 Ocean Dyn. 59(2), 227-238.
590 Beutler, M., Wiltshire, K.H., Reineke, C., Hansen, U.P., 2004. Algorithms and practical
591 fluorescence models of the photosynthetic apparatus of red cyanobacteria and
592 Cryptophyta designed for the fluorescence detection of red cyanobacteria and
593 cryptophytes. Aquatic Microbial Ecology 35(2), 115-129.
594 Beutler, M., Wiltshire, K.H., Meyer, B., Moldaenke, C., Lüring, C., Meyerhöfer, M., Hansen,
595 U.P., Dau, H., 2002. A fluorometric method for the differentiation of algal populations
596 in vivo and in situ. Photosynthesis Research 72(1), 39-53.

597 Bricaud, A., Babin, M., Morel, A., Claustre, H., 1995. Variability in the chlorophyll-specific
598 absorption-coefficients of natural phytoplankton - Analysis and parameterization.
599 Journal of Geophysical Research-Oceans 100(C7), 13321-13332.
600 Chekalyuk, A., Hafez, M., 2011. Photo-physiological variability in phytoplankton chlorophyll
601 fluorescence and assessment of chlorophyll concentration. Opt. Express 19(23),
602 22643-22658.
603 Cunningham, A., 1996. Variability of in-vivo chlorophyll fluorescence and its implications for
604 instrument development in bio-optical oceanography. Scientia Marina 60, 309-315.
605 Ducrotoy, J.P., Elliott, M., De Jonge, V.N., 2000. The North Sea. Mar. Pollut. Bull. 41(1-6), 5-
606 23.
607 Duysens, L.N., 1956. The flattening of the absorption spectrum of suspensions, as compared
608 to that of solutions. Biochimica et biophysica acta 19(1), 1-12.
609 Falkowski, P., Kiefer, D.A., 1985. Chlorophyll a fluorescence in phytoplankton: relationship to
610 photosynthesis and biomass. Journal of Plankton Research 7(5), 715-731.
611 Falkowski, P.G., Owens, T.G., 1980. Light—Shade Adaptation: Two strategies in marine
612 phytoplankton. Plant Physiology 66(4), 592-595.
613 Fleming, V., Kaitala, S., 2006. Phytoplankton spring bloom intensity index for the Baltic Sea
614 estimated for the years 1992 to 2004. Hydrobiologia 554(1), 57-65.
615 Fry, E.S., Kattawar, G.W., Pope, R.M., 1992. Integrating cavity absorption meter. Applied
616 Optics 31(12), 2055-2065.
617 Harvey, H.W., 1933. Measurement of phytoplankton population. Journal of the Marine
618 Biological Association of the United Kingdom 34, 761-774.
619 Hoepffner, N., Sathyendranath, S., 1991. Effect of pigment composition on absorption
620 properties of phytoplankton. Marine Ecology-Progress Series 73(1), 11-23.
621 Kiefer, D.A., 1973a. Fluorescence properties of natural phytoplankton populations. Marine
622 Biology 22(3), 263-269.
623 Kiefer, D.A., 1973b. Chlorophyll a fluorescence in marine centric diatoms: Responses of
624 chloroplasts to light and nutrient stress. Marine Biology 23(1), 39-46.

Kirk, J.T.O., 1994. Light & photosynthesis in aquatic ecosystems. 2 ed. Cambridge University Press, Cambridge, 509 pp.

Kirk, J.T.O., 1997. Point-source integrating-cavity absorption meter: Theoretical principles and numerical modeling. Applied Optics 36(24), 6123-6128.

Kirkpatrick, G. J., Millie, D.F., Moline, M.A., Lohrenz, S.E., Schofield O.M., 2011. Automated, in-water determination of colored dissolved organic material and phytoplankton community structure using the optical phytoplankton discriminator. Proceedings of SPIE - The International Society for Optical engineering 8030, art. no. 80300E.

Leathers, R.A., Downes, T.V., Davis, C.O., 2000. Analysis of a point-source integrating-cavity absorption meter. Applied Optics 39(33), 6118-6127.

Lips, I., Lips, U., Fleming, V., Kaitala, S., & Jaanus, A., 2007. Use of ferrybox measurements for the Baltic Sea environment assessment. Environmental Research, Engineering and Management 3(41), 3-8

Llewellyn, C.A., Gibb, S.W., 2000. Intra-class variability in the carbon, pigment and biomineral content of prymnesiophytes and diatoms. Marine Ecology-Progress Series 193, 33-44.

Llewellyn, C.A., Fishwick, J.R., Blackford, J.C., 2005. Phytoplankton community assemblage in the English Channel: a comparison using chlorophyll a derived from HPLC-CHEMTAX and carbon derived from microscopy cell counts. Journal of Plankton Research 27(1), 103-119.

Loftus, M. E., Seliger, H.H., 1975. Some limitations of the in vivo fluorescence technique. Chesapeake Science 16(2), 79-92.

Lorenzen, C.J., 1966. A method for the continuous measurement of in vivo chlorophyll concentration. Deep-Sea Research and Oceanographic Abstracts 13(2), 223-227.

Lutz, V.A., Sathyendaranath, S., Head, E.J.H., Li, W.K.W., 2001. Changes in the in vivo absorption and fluorescence excitation spectra with growth irradiance in three species of phytoplankton. Journal of Plankton Research 23(6), 555-569.

652 Mineeva, N.M., 2011. Plant pigments as indicators of phytoplankton biomass (review).
653 International Journal on Algae 13(4), 330-340.
654 Moore, C., Barnard, A., Fietzek, P., Lewis, M.R., Sosik, H.M., White, S., Zielinski, O., 2009.
655 Optical tools for ocean monitoring and research. Ocean Sci. 5(4), 661-684.
656 Morel, A., Bricaud, A., 1981. Theoretical results concerning light absorption in a discrete
657 medium, and application to specific absorption of phytoplankton. Deep Sea Research
658 Part A. Oceanographic Research Papers 28(11), 1375-1393.
659 Musser, J.A., Fry, E.S., Gray, D.J., 2009. Flow-through integrating cavity absorption meter:
660 experimental results. Applied Optics 48(19), 3596-3602.
661 Muylaert, K., Gonzales, R., Franck, M., Lionard, M., Van der Zee, C., Cattrijsse, A., Sabbe,
662 K., Chou, L., Vyverman, W., 2006. Spatial variation in phytoplankton dynamics in the
663 Belgian coastal zone of the North Sea studied by microscopy, HPLC-CHEMTAX and
664 underway fluorescence recordings. Journal of Sea Research 55(4), 253-265.
665 Ostrowska, M., Matorin, D.N., Ficek, D., 2000. Variability of the specific fluorescence of
666 chlorophyll in the ocean. Part 2. Fluorometric method of chlorophyll a determination.
667 Oceanologia 42(2), 221-229.
668 Parkhill, J.P., Maillet, G., Cullen, J.J., 2001. Fluorescence-based maximal quantum yield for
669 PSII as a diagnostic of nutrient stress. J. Phycol. 37(4), 517-529.
670 Pegau, W.S., Cleveland, J.S., Doss, W., Kennedy, C.D., Maffione, R.A., Mueller, J.L., Stone,
671 R., Trees, C.C., Weidemann, A.D., Wells, W.H., Zaneveld, J.R.V., 1995. A
672 comparison of methods for the measurement of the absorption coefficient in natural
673 waters. Journal of Geophysical Research-Oceans 100(C7), 13201-13220.
674 Petersen, W., Schroeder, F., Bockelmann, F.D., 2011. FerryBox - Application of continuous
675 water quality observations along transects in the North Sea. Ocean Dyn. 61(10),
676 1541-1554.
677 Petersen, W., Wehde, H., Krasernann, H., Colijn, F., Schroeder, F., 2008. FerryBox and
678 MERIS - Assessment of coastal and shelf sea ecosystems by combining in situ and
679 remotely sensed data. Estuarine Coastal and Shelf Science 77(2), 296-307.

680 Pope, R.M., Weidemann, A.D., Fry, E.S., 2000. Integrating Cavity Absorption Meter
681 measurements of dissolved substances and suspended particles in ocean water.
682 Dynamics of Atmospheres and Oceans 31(1-4), 307-320.
683 Prézelin, B.B., Ley, A.C., 1980. Photosynthesis and chlorophyll a fluorescence rhythms of
684 marine phytoplankton. Marine Biology 55(4), 295-307.
685 Reid, P.C., Colebrook, J.M., Matthews, J.B.L., Aiken, J., Continuous Plankton Recorder, T.,
686 2003. The Continuous Plankton Recorder: concepts and history, from plankton
687 indicator to undulating recorders. Prog. Oceanogr. 58(2-4), 117-173.
688 Reuter, R., Badewien, T.H., BartholomÄ, A., Braun, A., Lübben, A., Rullkötter, J., 2009. A
689 hydrographic time series station in the Wadden Sea (southern North Sea). Ocean
690 Dyn. 59(2), 195-211.
691 Röttgers, R., Doerffer, R., 2007. Measurements of optical absorption by chromophoric
692 dissolved organic matter using a point-source integrating-cavity absorption meter.
693 Limnology and Oceanography-Methods 5, 126-135.
694 Röttgers, R., Schönfeld, W., Kipp, P.R., Doerffer, R., 2005. Practical test of a point-source
695 integrating cavity absorption meter: the performance of different collector assemblies.
696 Applied Optics 44(26), 5549-5560.
697 Schlitzer, R., 2011. Ocean Data View. http://odv.awi.de
698 Seppälä, J., Balode, M., 1998. The use of spectral fluorescence methods to detect changes
699 in the phytoplankton community. Hydrobiologia 363, 207-217.
700 Soohoo, J.B., Kiefer, D.A., Collins, D.J., McDermid, I.S., 1986. In vivo fluorescence excitation
701 and absorption spectra of marine phytoplankton: I. Taxonomic characteristics and
702 responses to photoadaptation. Journal of Plankton Research 8(1), 197-214.
703 Stavn, R.H., Rick, H.J., Falster, A.V., 2009. Correcting the errors from variable sea salt
704 retention and water of hydration in loss on ignition analysis: Implications for studies of
705 estuarine and coastal waters. Estuarine, Coastal and Shelf Science 81(4), 575-582.

706 Sternberg, R.W., Baker, E.T., McManus, D.A., Smith, S., Morrison, D.R., 1974. An integrating
707 nephelometer for measuring particle concentrations in the deep sea. Deep-Sea
708 Research and Oceanographic Abstracts 21(10), 887-892.
709 Stramski, D., Babin, M., Wozniak, S.B., 2007. Variations in the optical properties of
710 terrigenous mineral-rich particulate matter suspended in seawater. Limnol. Oceanogr.
711 52(6), 2418-2433.
712 Szabo, I., Bergantino, E., Giacometti, G.M., 2005. Light and oxygenic photosynthesis: energy
713 dissipation as a protection mechanism against photo-oxidation. Embo Reports 6(7),
714 629-634.
715 TurnerDesigns, 2004. SCUFA user´s manual.
716 http://www.turnerdesigns.com/t2/doc/manuals/998-2002.pdf. Accessed 22.04.13
717 Uehlinger, U., 1985. An in situ pulse light fluorometer for chlorophyll determination as a
718 monitor for vertical and horizontal phytoplankton distribution in lakes. Journal of
719 Plankton Research 7(5), 605-615.
720 Vant, W.N., 1990. Causes of light attenuation in nine New Zealand estuaries. Estuarine,
721 Coastal and Shelf Science 31(2), 125-137.
722 Wiltshire, K.H., Harsdorf, S., Smidt, B., Blöcker, G., Reuter, R., Schroeder, F., 1998. The
723 determination of algal biomass (as chlorophyll) in suspended matter from the Elbe
724 estuary and the German Bight: A comparison of high-performance liquid
725 chromatography, delayed fluorescence and prompt fluorescence methods. Journal of
726 Experimental Marine Biology and Ecology 222(1-2), 113-131.
727 Wiltshire, K.H., Kraberg, A., Bartsch, I., Boersma, M., Franke, H.D., Freund, J., Gebühr, C.,
728 Gerdts, G., Stockmann, K., Wichels, A., 2010. Helgoland Roads, North Sea: 45 Years
729 of Change. Estuaries Coasts 33(2), 295-310.
730 Wollschläger, J., Grunwald, M., Röttgers, R., Petersen, W., 2013. Flow-through PSICAM: a
731 new approach for determining water constituents absorption continuously. Ocean
732 Dyn. 63(7), 761-775.

733 Wozniak, S.B., Stramski, D., Stramska, M., Reynolds, R.A., Wright, V.M., Miksic, E.Y.,
734 Cichocka, M., Cieplak, A.M., 2010. Optical variability of seawater in relation to particle
735 concentration, composition, and size distribution in the nearshore marine environment
736 at Imperial Beach, California. Journal of Geophysical Research C: Oceans 115(8).
737 Wright, S.W., Jeffrey, S.W., Mantoura, R.F.C., Llewellyn, C.A., Bjørnland, T., Repeta, D.
738 Welschmeyer, N., 1991. Improved HPLC method for the analysis of chlorophylls and
739 carotenoids from marine phytoplankton. Marine Ecology Progress Series 77(2-3),
740 183-196.
741 Yentsch, C.S., Yentsch, C.M., 1979. Fluorescence spectral signatures: The characterization
742 of phytoplankton populations by the use of excitation and emission spectra. Journal of
743 Marine Research 37(3), 471-483.
744 Yentsch, C.S., Phinney, D.A., 1989. A bridge bewteen ocean optics and microbial ecology.
745 Limnology & Oceanography 34(8), 1649-1705.
746 Zapata, M., Rodriguez, F., Garrido, J.L., 2000. Separation of chlorophylls and carotenoids
747 from marine phytoplankton: a new HPLC method using a reversed phase C-8 column
748 and pyridine-containing mobile phases. Marine Ecology-Progress Series 195, 29-45.
749
750